

Absolute Configuration and Conformation Analysis of 1-Phenylethanol by Matrix-Isolation Infrared and Vibrational Circular Dichroism Spectroscopy Combined with Density Functional Theory Calculation

Kei Shin-ya,[†] Hiromu Sugeta,[†] Saeko Shin,[‡] Yoshiaki Hamada,[‡] Yukiteru Katsumoto,^{*,†} and Keiichi Ohno[†]

Graduate School of Science, Hiroshima University, 1-3-1 Kagamiyama, Higashi-Hiroshima 739-8526, Japan, and The University of the Air, Chiba 261-8686, Japan

Received: December 8, 2006; In Final Form: June 4, 2007

The absolute configuration and conformation of 1-phenylethanol (1-PhEtOH) have been determined by matrix-isolation infrared (IR) and vibrational circular dichroism (VCD) spectroscopy combined with quantum chemical calculations. Quantum chemical calculations have identified that there are three conformers, namely, I, II, and III, in which characteristic intramolecular interactions are found. The IR spectrum–conformation correlation for 1-PhEtOH has been developed by the Ar matrix-isolation IR measurement and used for the assignments of the observed IR bands. In a dilute CCl₄ solution, 1-PhEtOH exists predominantly as conformer I along with a trace amount of conformer II. By considering conformations and intermolecular hydrogen-bonding in the spectral simulation for (*S*)-1-PhEtOH, we have successfully reproduced the VCD spectrum of (–)-1-PhEtOH observed in a dilute CS₂ solution. Thus, (–)-1-PhEtOH is of *S*-configuration and conformer I in the dilute solution. The same method has been applied to analyze the VCD spectra measured in the liquid state of (–)-1-PhEtOH. The absolute configuration of 1-PhEtOH in the condensed phase is enabled by identifying VCD bands that are insensitive to conformational changes and intermolecular interactions. The present work provides a combinatorial procedure for determination of both the absolute configuration and the conformation of chiral molecules in a dilute solution and condensed phase.

Introduction

Absolute configurations and conformations of chiral molecules are closely related to their physical and chemical properties and play an important role in biological activities.^{1–7} The absolute configurations have most often been determined by X-ray diffraction.⁸ Since the X-ray diffraction study requires single-crystal samples, an alternative technique is desirable in order to determine absolute configurations of molecules in solutions. Vibrational circular dichroism (VCD) spectroscopy is now known as the alternative technique for determining the absolute configurations of chiral molecules as well as their conformations.^{9–11} However, when a chiral molecule has several conformers, interpretation of its VCD spectrum is not straightforward. On the other hand, the matrix-isolation infrared (IR) spectroscopy combined with theoretical calculations can determine the conformations of isolated molecules with negligible intermolecular interactions in a low-temperature matrix.^{12–14} Thus, an IR spectrum–conformation correlation established by the matrix-isolation IR spectroscopy should be very useful to analyze VCD spectra for determining both the absolute configuration and conformation of a chiral molecule.

1-PhEtOH is a simple chiral molecule, which has several conformations in the solution and in the liquid state. Mass-selected resonant two-photon ionization (R2PI) and IR–UV measurements for 1-PhEtOH in a supersonic jet have revealed that only one stable conformer exists, in which the OH group

slightly interacts with the phenyl ring.^{15,16} Recently, Macleod et al.^{17,18} have investigated the conformation of 1-PhEtOH in the liquid state by the use of electronic circular dichroism (ECD) and Raman optical activity (ROA) combined with theoretical calculations. They reported that the calculated ROA spectrum in the region below 1120 cm^{–1} is in excellent agreement with that observed in the liquid state, whereas that in 1120–1400 cm^{–1} region is not. Since the bands in the 1120–1400 cm^{–1} region are involved in the OH bending mode, the discrepancy may arise from the intermolecular interactions of 1-PhEtOH. Thus, it is of interest to obtain a deeper insight into conformations and molecular interactions of 1-PhEtOH through the IR and VCD measurements in the matrix, the dilute solution, and the liquid state.

In the present work, we have determined the absolute configuration and conformation of 1-PhEtOH in solutions by the following procedures. First, we obtained the local minima of (*S*)-1-PhEtOH on the two-dimensional (2-D) potential-energy surface using an ab initio Hartree–Fock (HF) method. Then, the conformer for each local minimum was optimized by the density functional theory (DFT) calculation, and their IR and VCD spectra were calculated. Second, the conformer of 1-PhEtOH in the Ar matrix was determined by comparing the matrix-isolation IR spectra with the calculated spectra, and an IR spectrum–conformation correlation was obtained. Third, conformations of 1-PhEtOH in dilute CCl₄ and CS₂ solutions were determined using the IR spectrum–conformation correlation. Finally, the absolute configuration of (–)-1-PhEtOH in the solutions was determined by VCD spectroscopy. The VCD spectrum in the liquid state was also examined by considering

* Corresponding author. E-mail: katsumot@hiroshima-u.ac.jp. Tel.: +81-82-424-7408. Fax: +81-82-424-0727.

[†] Hiroshima University.

[‡] The University of the Air.

both conformations and intermolecular OH...O hydrogen bonding (H-bonding). This procedure successfully determined the absolute configurations and conformations of chiral molecules that have several conformers in solutions and in the liquid state.

Experimental Section

Sample Preparation. DL- and (–)-1-PhEtOH were purchased from Tokyo Kasei Kogyo. The chemical and enantiometric purities of the (–)-1-PhEtOH sample were over 98%. The matrix-isolation IR spectra were recorded on a JASCO FT/IR-615 Fourier transform spectrometer equipped with a DTGS detector by coaddition of 100 scans at a resolution of 1 cm⁻¹. Premixed gas of Ar/sample = 2000 was slowly sprayed onto a CsI plate cooled to 12 K by an Iwatani Cryomini D510 refrigerator. The deposited sample was annealed at different temperatures from 12 to 41 K in order to examine the temperature dependence on conformational equilibrium.

IR and VCD Measurements. The IR spectra of (–)-1-PhEtOH in CCl₄, CS₂, and benzene solutions and in a liquid state were recorded on a JASCO FT/IR-620 Fourier transform spectrometer equipped with a DTGS detector by coaddition of 100 scans at a resolution of 2 cm⁻¹. The VCD spectra of (–)-1-PhEtOH in a CS₂ solution and a liquid state were recorded on a Bomem-BioTools Fourier transform VCD spectrometer with a data correction time of 2 h at a resolution of 4.0 cm⁻¹.

Calculations. Theoretical calculations were performed with the Gaussian 03 program.¹⁹ The ab initio MO calculation at the HF/6-31G(d,p) level was used to develop the 2-D potential-energy surface map for (S)-1-PhEtOH. To obtain the molecular structure at local minima, we performed the structural optimization by DFT calculations at the B3LYP/6-31+G(d,p) and B3LYP/6-311++G(d,p) levels²⁰ and ab initio MO calculation with the Møller–Plesset second perturbation (MP2) theory with the 6-31+G(d,p) basis set.²¹ The effects of solvation on the optimized geometry and energy of 1-PhEtOH were examined by means of the self-consistent reaction field (SCRF) theory with integral equation formalism–polarizable continuum model (IEF–PCM) at the B3LYP/6-31+G(d,p) level.²² Gibbs free energy for each conformer was calculated by the G2MP2 method.²³ For the calculations of dimers of (S)-1-PhEtOH, the DFT calculations at the B3LYP/6-31+G(d,p) level were carried out. The optimized structures, relative energies with the zero-point energy correction, harmonic vibrational wavenumbers ν_{harm} , absorption IR and VCD intensities, and potential-energy barriers were obtained for the conformers of (S)-1-PhEtOH. The wavenumber-linear scaling (WLS) scaling with $\nu_{\text{cal}}/\nu_{\text{harm}} = 1 - 0.0001838\nu_{\text{harm}}$ is applied for the calculated IR wavenumbers in the fingerprint region,²⁴ and a single scaling factor of 0.945 is used for the OH stretching wavenumbers. The IR spectra of (S)-1-PhEtOH were simulated by assuming a Lorentzian-type band shape with the full bandwidths at the half-height of 1 cm⁻¹ for the Ar matrix and 10 cm⁻¹ for the solutions and the liquid state.

Results and Discussion

Relative Energies of Conformers. Figure 1 shows the contour map of the 2-D potential-energy surface of (S)-1-PhEtOH calculated at the HF/6-31G(d,p) level as a function of the C₁C_α–OH and C₂C₁–C_αO dihedral angles (see Figure 2 for the definitions of the dihedral angles). The conformers corresponding to the three local minima I, II, and III were optimized at the B3LYP/6-311++G(d,p) level. Figure 2 shows the three optimized conformers of (S)-1-PhEtOH. The relative energies with the zero-point energy correction for conformers I, II, and III are calculated to be 0.00, 4.73, and 7.25 kJ mol⁻¹,

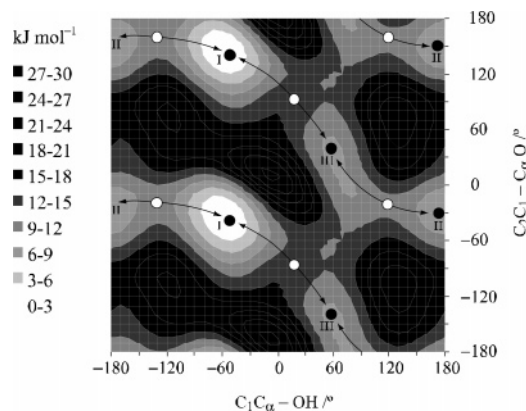


Figure 1. Contour map of the 2-D potential-energy surface for (S)-1-PhEtOH against dihedral angles C₂C₁–C_αO and C₁C_α–OH at the HF/6-31G(d,p) level. Successive contour plots differ by 3 kJ mol⁻¹; ●, local minima of conformers I, II, and III; ○, transition states.

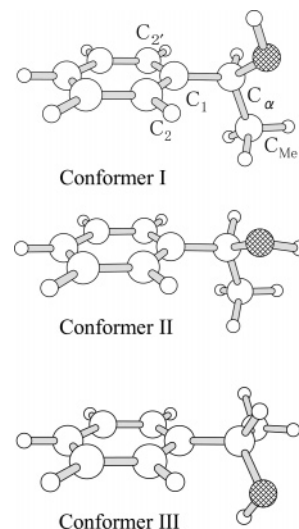


Figure 2. Conformers I, II, and III of (S)-1-PhEtOH optimized at the B3LYP/6-311++G(d,p) level.

respectively. The dihedral angles and relative energies of the conformers are listed in Table 1. The C₂C₁–C_αC and C₂C₁–C_αO dihedral angles (77° and –43°) of the most stable conformer I are similar to those (90° and –51°) of the most stable conformers of ethyl benzene²⁵ and benzyl alcohol.²⁶ The geometry of each conformer optimized at the MP2/6-31+G(d,p) level is similar to that obtained at the B3LYP/6-311++G(d,p) level,²⁷ and the relative energy ordering of conformers does not change in both the methods. By performing the IEF–PCM method at the B3LYP/6-31+G(d,p) level, we confirmed that the effect of polar (methanol) and nonpolar (CCl₄) solvents on the structure and relative energy of conformers is not significant.²⁸ These relative energies are compiled in Table 1, together with Gibbs free energy for each conformer estimated by the G2MP2 method. As shown in Table 1, the relative energy ordering of conformers is conserved for all calculation methods: conformer I is the most stable, whereas conformer III is the least.

The contribution of intramolecular interactions on the optimized structure has been examined in terms of the optimized geometries at the B3LYP/6-311++G(d,p). The OH bonds of conformers I and III are directed to the phenyl ring, while the OH bond of conformer II is on the opposite side to the phenyl ring. The calculated OH bond length of conformer I (96.3 pm) or III (96.4 pm) is longer by about 0.1 or 0.2 pm than that of conformer II (96.2 pm), indicating that conformers I and III

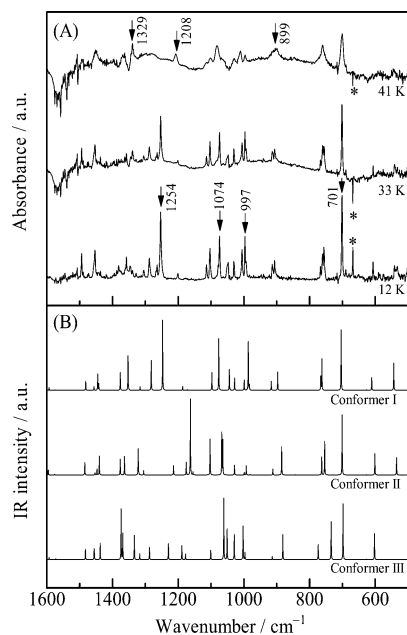


Figure 3. (A) IR spectra of DL-1-PhEtOH in the Ar matrix annealed at 12, 33, and 41 K. (B) Calculated IR spectra of conformers I, II, and III. An asterisk symbol (*) indicates the band due to CO₂.

are likely to be stabilized by intramolecular OH $\cdots\pi$ H-bonding. On the other hand, the O \cdots H distances between the hydroxyl O and H(C₂) atoms are calculated to be 269.9, 242.7, and 264.3 pm for conformers I, II, and III, respectively. The results imply the existence of an attractive intramolecular CH \cdots O H-bond, because they are shorter than the sum of the van der Waals radii of H and O (270 pm).^{12–14} The bond lengths of the C₂–H group are estimated to be 108.4, 108.2, and 108.4 pm for conformers I, II, and III, respectively. The bond length of the H-bonded C₂–H group in conformer I or II is shorter by about 0.3 pm than that of the C₂–H group (108.6 pm) that does not form an intramolecular CH \cdots O H-bond. A shortened C–H bond is often found in CH \cdots O H-bonding.²⁹

The calculation results imply that conformer I is stabilized by both intramolecular OH $\cdots\pi$ and CH \cdots O H-bonding. Conformer II is stabilized only by intramolecular CH \cdots O H-bonding and is less stable by 4.73 kJ mol⁻¹ than conformer I. Conformer III is the least stable, though it possesses intramolecular OH $\cdots\pi$ and CH \cdots O H-bonding. Although the C₂C₁–C _{α} C dihedral angle prefers ca. 90° for ethylbenzene as determined by microwave spectroscopy,³⁰ that for conformer III is estimated to be –6° (Table 1). Thus, we interpreted that the destabilization

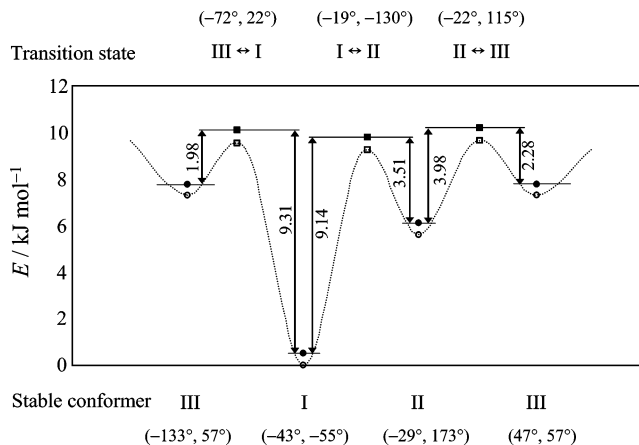


Figure 4. Schematic diagram of barrier heights between the conformers of (*S*)-1-PhEtOH calculated at the B3LYP/6-311++G(d,p) level. Dihedral angles (C₂C₁–C _{α} O, C₁C _{α} –OH) of the conformers optimized are given in parentheses. Energies at local minima and maxima are represented by open circle and square symbols, respectively. Filled symbols are used for the energies with zero-point energy correction.

of conformer III is caused by the steric repulsion between the H(C₂) atom of the phenyl ring and the H atoms of the methyl group.

Matrix-Isolation IR Spectra. The Ar matrix-isolation IR spectra of DL-1-PhEtOH in the 1600–500 cm⁻¹ region are shown in Figure 3, along with the calculated spectra of conformers I, II, and III. The brief assignments of the observed and calculated IR bands are compiled in Table 2. As shown in Figure 3, the calculated spectrum of conformer I reproduces very well the matrix IR spectra observed at 12 and 33 K. Thus, we concluded that conformer I persists predominantly in the Ar matrix at 12 and 33 K. The dominant bands observed at 1254, 1074, 997, and 701 cm⁻¹ are assigned to the COH bending, C–O stretching, CH₃ rocking, and out-of-plane ring deformation of conformer I, respectively. The exclusive existence of conformer I in the Ar matrix is consistent with the results of the R2PI and IR–UV experiments in supersonic beams.^{15,16} On annealing the deposited sample, the sharp bands retaining their relative intensities up to 33 K change to liquid-like bands at 41 K owing to the evaporation of Ar. The bands at 1329, 1208, and 899 cm⁻¹, which increase in intensity at 41 K, are possibly associated with conformer II. Conformer II may be stabilized by the intermolecular OH \cdots O H-bond occurring in the condensed phase as described later.

The population of conformers frozen in a low-temperature matrix can be assumed to be the same as that of the vapor sample just before the deposition.^{31,32} In order to measure the

TABLE 1: Relative Energies of Conformers of (*S*)-1-PhEtOH Calculated at the B3LYP/6-311++G(d,p) Level

conformer	dihedral angle ^a			energy/kJ mol ⁻¹						
	C ₂ C ₁ –C _{α} C (deg)	C ₂ C ₁ –C _{α} O (deg)	C ₁ C _{α} –OH (deg)	B3LYP ^b			ΔG^c	PCM ^{b,d}		interaction
				6-311++G(d,p)	6-31+G(d,p)	6-31+G(d,p)		CCl ₄	methanol	
I	77	–43	–55	0.00	0.00	0.00	0.00	0.00	0.00	OH $\cdots\pi$ H-bond CH \cdots O H-bond
II	93	–29	173	4.73	4.77	5.36	3.41	4.50	3.86	CH \cdots O H-bond
III	–6	47	57	7.25	7.26	10.07	7.62	7.35	7.06	CH \cdots H _{Me} repulsion OH $\cdots\pi$ H-bond CH \cdots O H-bond

^a The notation of dihedral angles is shown in Figure 2. The value of the C₂C₁–C _{α} C angle of ethyl benzene is 90°, and the values of the C₂C₁–C _{α} O and C₁C _{α} –OH angles of benzyl alcohol are –51° and –56°, respectively (refs 21 and 22). ^b Relative energy with the zero-point energy correction. ^c Gibbs free energy estimated by the G2MP2 method. ^d The energy is estimated by means of the IEF–PCM at the B3LYP/6-31+G(d,p) level of calculation using the CCl₄ or methanol solvent parameters.

TABLE 2: Calculated and Observed Wavenumbers and Vibrational Assignments of 1-PhEtOH in the 1600–500 cm⁻¹ Region

Ar matrix	observed			calculated					
	int. ^a	liquid	int. ^a	conformer I	int./km mol ⁻¹	assignment ^b	conformer II	int./km mol ⁻¹	assignment ^b
1495	s	1493	s	1482	6	C=C str	1484	9	C=C str
				1456	3	CH ₃ a-def	1453	2	CH ₃ a-def
1454	s	1451	s	1445	11	CH ₃ a-def	1447	4	CH ₃ a-def
				1442	5	C=C str	1440	13	C=C str
1382	vw								
1358	w	1369	m	1376	13	CH ₃ s-def	1376	11	CH def
1347	w	1353	vw	1353	24	CH def	1364	14	CH ₃ s-def
1339	vw			1351	2	CH def			
1329	w	1327	vw				1322	19	CH def
1306	w	1304	vw	1316	3	C=C str	1320	1	CH bend (ip)
1288	m	1284	vw	1282	22	CH bend (ip)	1305	3	C=C str
1267	vw								
1264	vw								
1254	vs	1259	vw	1248	50	COH bend			
		1204	s				1214	7	φ-C str
1208	w			1186	3	φ-C str			
		1178	w	1173	0	CH bend (ip)	1163 ^c	54	COH bend
		1156	w	1156	0	CH bend (ip)	1176	9	CH bend (ip)
							1155	2	CH bend (ip)
1115	m	1113	sh						
1103	s	1099	m	1097	13	CH bend (ip)	1103	25	C–O str
1074	s	1077	vs	1077	37	C–O str	1067	30	CH ₃ rock
		1058	sh				1064	25	CH bend (ip)
1049	m			1044	15	CH ₃ rock			
1031	m	1029	m	1028	9	CH bend (ip)	1029	7	CH bend (ip)
1006	s	1011	s	999	8	C=C str	999	2	C=C str
997	s	997	m	987	35	CH ₃ rock	993	7	CH ₃ rock
993	w			983	4	CH bend (op)	981	0	CH bend (op)
		968	vw	969	0	CH bend (op)	965	0	CH bend (op)
914	m	911	sh	917	7	CH bend (op)	912	4	CH bend (op)
907	m	899	s	897	14	C–C str	885	21	C–C str
		845	vw	847	0	CH bend (op)	844	0	CH bend (op)
767	w								
761	s			766	10	φ-C str			
756	s	760	s	763	22	CH bend (op)	763	13	φ-C str
		740	sh				754	24	CH bend (op)
701	vs	699	vs	704	45	φ def (op)	701	45	φ def (op)
				627	0	φ def (ip)	627	0	φ def (ip)
607	m	607	m	611	9	φ def (ip)	601	15	φ def (ip)
541	w	538	m	544	19	φ def (op)	535	12	φ def (op)
533	w								

^a int., intensity; vs, very strong; s, strong; m, medium; w, weak; vw, very weak; sh, shoulder. ^b CH bend, CH bending of the phenyl ring; CH₃ a-def, CH₃ asymmetric deformation; CH₃ s-def, CH₃ symmetric deformation; CH def, CH deformation of the CH group; C=C str, C=C stretching; COH bend, COH bending; C–O str, C–O stretching; CH₃ rock, CH₃ rocking; C–C str, C–C stretching; φ def, deformation of the phenyl ring; ip, in-plane mode; op, out-of-plane mode. ^c The band may be shifted to a higher wavenumber at ca. 1400 cm⁻¹ by forming intermolecular hydrogen bonding in the liquid state. See text.

spectrum of less stable conformers, the temperature of the premixed gas was set at 398 and 498 K before depositing onto a CsI plate kept at 12 K. However, the obtained spectra were found to be almost the same as those in Figure 3, suggesting that the barrier heights between the conformers should be low. Figure 4 shows the energies of the local maxima (transition states) and local minima (stable conformers) of (*S*)-1-PhEtOH calculated at the B3LYP/6-311++G(d,p) level. The barrier heights from conformer II to I, III to I, and III to II are calculated to be 3.51, 1.98, and 2.28 kJ mol⁻¹, respectively. These barriers are low enough to permit the conformational change even at 12 K on the basis of the Arrhenius equation with the *A* factor given by Barnes.³³ On the contrary, the barrier heights from conformer I to III and I to II are found to be 9.31 and 9.14 kJ mol⁻¹, respectively. These calculations imply that the conformational change from conformer II or III to I is almost irreversible. Consequently, the population of conformer I is predominant in a low-temperature matrix. The calculation supports the experimental result that no strong bands due to conformers II and III are observed in the Ar matrix immediately after the deposition.

Absorption IR Spectra in Solutions and the Liquid State.

Figure 5 shows the absorption IR spectra of (–)-1-PhEtOH in the 1600–500 cm⁻¹ region along with the calculated spectra. Note that these spectra were represented after the subtraction of a solvent spectrum. The IR spectrum of (–)-1-PhEtOH in a CS₂ solution at a concentration of 0.01 mol dm⁻³ (M) is similar to that in the Ar matrix represented in Figure 3 except the bandwidths. However, in the CS₂ solution of (–)-1-PhEtOH, several weak bands were additionally observed at 1204, 1178, 1156, and 740 cm⁻¹, which are associated with conformer II as listed in Table 2. The relative intensities of these bands increase with increasing concentration. It is worth noting that the increase in the relative intensities of the bands at 1011, 899, and 607 cm⁻¹ is also observed. This tendency is observed also in the annealing process of the Ar matrix; the intensities of the bands at 1329, 1208, and 899 cm⁻¹ tend to be stronger in the spectrum annealed at 41 K (Figure 3).

A remarkable change in the relative intensities was observed for the bands at 1251 and 1204 cm⁻¹. The intensity of the band at 1251 cm⁻¹ decreases and that of the 1204 cm⁻¹ band increases with increasing concentration as can be seen in Figure 5A. In

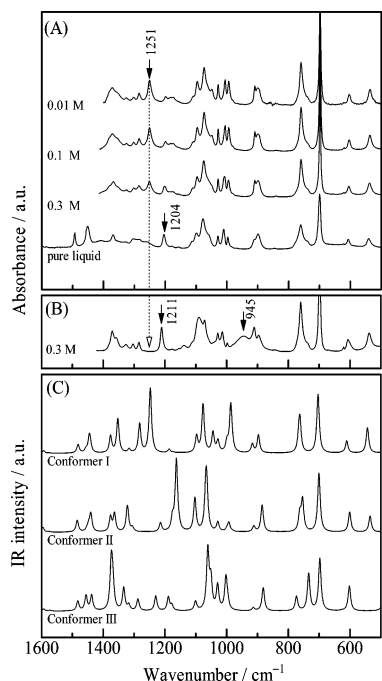


Figure 5. (A) Absorption IR spectra of (–)-1-PhEtOH observed at 0.01, 0.10, and 0.30 M in CS₂ solutions and that for the pure liquid. (B) The IR spectrum of 1-PhEtOD in the 0.3 M CS₂ solution. (C) Calculated IR spectra for conformers I, II, and III.

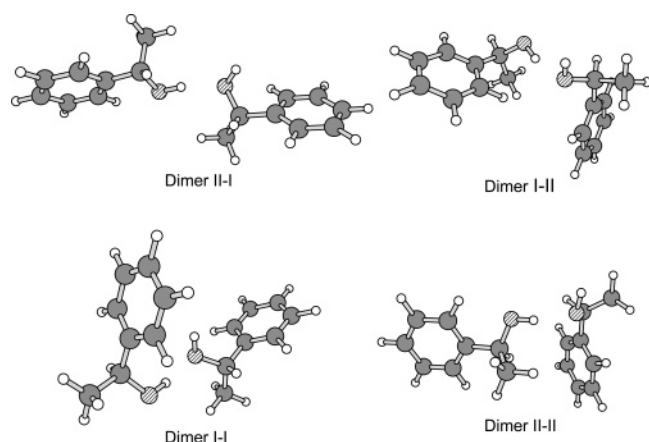


Figure 6. Structures of the dimers of (S)-1-PhEtOH optimized at the B3LYP/6-31+G(d,p) level.

the calculated spectra, the COH bending band is estimated to be at 1248 cm⁻¹ for conformer I. In order to confirm the assignment of the COH bending band, the IR spectrum of deuterated species PhEtOD was measured. Figure 5B shows the IR spectrum of PhEtOD in a CS₂ solution at 0.3 M. The 1251 cm⁻¹ band is shifted to 945 cm⁻¹ upon the deuteration, whereas the fairly strong band is still observed at 1211 cm⁻¹. Thus, the band at 1251 cm⁻¹ is definitely assigned to the COH bending of conformer I.

The assignment of the band at 1204 cm⁻¹ is unlikely due to the monomer of (–)-1-PhEtOH, because no corresponding band is found in the calculated IR bands for conformers I, II, and III listed in Table 2. Therefore, we presumed that the band at 1204 cm⁻¹ arises from an intermolecular H-bonding. To investigate the influence of the intermolecular H-bonding on the IR bands, we performed the quantum chemical calculations for dimers of (S)-1-PhEtOH at the B3LYP/6-31+G(d,p) level. The optimized structures of the dimers are shown in Figure 6: dimer I–I composed of conformer I, dimer II–II composed of conformer II, dimer II–I composed of conformer II (donor) and conformer

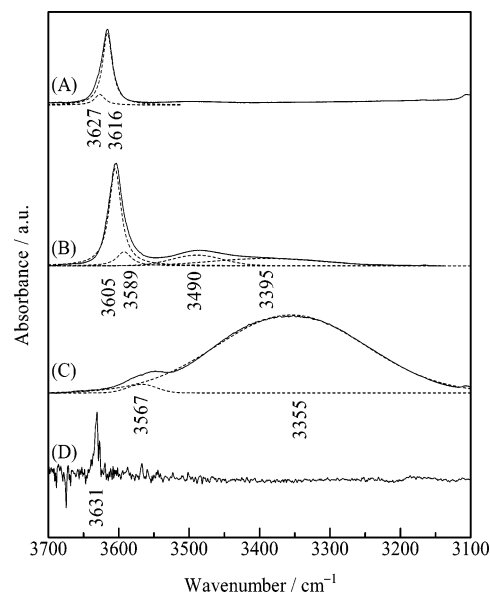


Figure 7. Observed IR spectra of 1-PhEtOH in the ν_{OH} region: (A) the CCl₄ solution at 0.01 M; (B) the CS₂ solution at 0.1 M; (C) the liquid state; (D) the Ar matrix. The results of curve fitting are represented by dotted lines.

I (acceptor), and dimer I–II composed of conformer I (donor) and conformer II (acceptor). The results revealed that the H-bonded COH bending band of conformers I and II shifts to a higher wavenumber and appears at 1390–1420 cm⁻¹. Interestingly, the phenyl-C (ϕ -C) stretching band of conformer II slightly shifts to a lower frequency (appears at ca. 1200 cm⁻¹) and its intensity increases in dimers. Thus, the band observed at 1204 cm⁻¹ is assignable to the ϕ -C stretching band of conformer II with OH \cdots O H-bonding.

Based on the assignments, we concluded that the concentration-dependent changes in the relative intensity of the IR bands are caused by the conformational change from conformer I to II. The increase in population of conformer II for the concentrated solution of (–)-1-PhEtOH suggests that conformer II is stabilized by intermolecular OH \cdots O H-bonding. As a result, conformer I exists predominantly in the dilute solution of (–)-1-PhEtOH along with a trace amount of conformer II, whereas conformer II is dominant in the liquid state.

OH Stretching Band. OH stretching (ν_{OH}) bands give useful information concerning H-bonds and conformations around a CC–OH bond.³⁴ Figure 7 shows the IR spectra in the ν_{OH} region of 1-PhEtOH. The ν_{OH} band is observed at 3631 and 3616 cm⁻¹ in the Ar matrix and the CCl₄ solution, respectively (Figure 7, parts D and A). Note that in a supersonic jet the ν_{OH} band of 1-PhEtOH is located at 3647 cm⁻¹.¹⁶ The OH wavenumbers observed in the Ar matrix or in the CCl₄ solution are lower than that in the gas phase, because of the interactions of the ν_{OH} bond with surrounding molecules.³⁵ As shown in Figure 7A, the ν_{OH} band for 1-PhEtOH in CCl₄ is asymmetric with a tail toward higher wavenumbers. The envelope was reasonably decomposed into two components at 3616 and 3627 cm⁻¹ with the band-intensity ratio of 1:0.16. In a previous section, the IR analysis in the 1600–500 cm⁻¹ region indicates that conformer I exists predominantly in the dilute solution along with conformer II as a minor component. Thus, it is likely that the main band at 3616 cm⁻¹ is associated with conformer I, whereas the sub-band at 3627 cm⁻¹ is concerned with conformer II.

The ν_{OH} band due to conformer I is lower by 11 cm⁻¹ than that arising from conformer II. This may be caused by the intramolecular OH \cdots π H-bond. The ν_{OH} wavenumbers for

conformers I, II, and III are calculated to be 3613, 3630, and 3598 cm^{-1} , respectively. The O–H bond lengths for conformers I, II, and III are 96.3, 96.2, and 96.4 pm, respectively. In general, the O–H bond lengths are inversely proportional to their wavenumbers.³⁶ The calculation results indicate that the $\text{OH}\cdots\pi$ H-bond causes a lower wavenumber shift of the ν_{OH} band of conformer I by 17 cm^{-1} . Therefore, we concluded that the main band at 3616 cm^{-1} is due to the ν_{OH} band of conformer I with the intramolecular $\text{OH}\cdots\pi$ H-bond and the weak sub-band observed at 3627 cm^{-1} arises from the free ν_{OH} of conformer II. By using the absorption coefficient (α) and energy difference ΔE between conformers I and II calculated at the B3LYP/6-311++G(d,p) level with the zero-point correction, the IR absorption intensity ratio between IR bands of conformers can be estimated by following equation: $(A_{\text{II}}/A_{\text{I}})_{\text{calc}} = (\alpha_{\text{II}}N_{\text{II}}/\alpha_{\text{I}}N_{\text{I}}) = (\alpha_{\text{II}}/\alpha_{\text{I}}) \exp(-\Delta E/RT)$. The $(A_{\text{II}}/A_{\text{I}})_{\text{calc}}$ obtained was 0.16 at 300 K, which is in excellent harmony with the experimental value 0.16.

As shown Figure 7C, the ν_{OH} band envelope for 1-PhEtOH in the liquid state was decomposed into two bands at 3355 and about 3567 cm^{-1} with the band-intensity ratio of 1:0.02. According to the relationship between the H-bonding pattern and the ν_{OH} wavenumber previously reported,³⁷ the main 3355 cm^{-1} band is assignable to the intermolecular H-bonded ν_{OH} mode in the two-coordinated H-bonding networks. To assign the weak band at 3567 cm^{-1} , we considered the intermolecular $\text{OH}\cdots\pi$ interaction. The ν_{OH} band of 1-PhEtOH was observed at 3588 cm^{-1} in a benzene solution and at 3616 cm^{-1} in a CCl_4 solution. Similar observations have been reported for 1-octanol (3632 and 3611 cm^{-1} in benzene and 3642 and 3635 cm^{-1} in CCl_4) and ethanol (3613 and 3603 cm^{-1} in benzene and 3638 and 3633 cm^{-1} in CCl_4).³⁸ The significant red-shift of the ν_{OH} band in benzene solution is attributed to the interaction between the OH group and the delocalized electronic structure of benzene. The ν_{OH} band at 3567 cm^{-1} has been characteristically observed in the liquid state for phenyl alcohols but not observed for aliphatic alcohols.³⁹ Therefore, we concluded that the band at 3567 cm^{-1} for 1-PhEtOH in the liquid state originates from the intermolecular $\text{OH}\cdots\pi$ H-bond.

Figure 7B shows the ν_{OH} envelop for 1-PhEtOH in a CS_2 solution at 0.1 M, which seems to possess both the features of the ν_{OH} band observed in CCl_4 and in the liquid state. The characteristic band observed at 3490 cm^{-1} is due to a dimer of 1-PhEtOH. The bands at 3616 and 3355 cm^{-1} arise for the monomer and multimer, respectively. The above experimental results indicate that in the liquid state the OH bonds of 1-PhEtOH mainly form the intermolecular two-coordinated H-bonding networks composed of conformers I and II, and the minority is involved in the intermolecular $\text{OH}\cdots\pi$ H-bonding. The analysis of the ν_{OH} band has also shown that conformer I exists predominantly in the CCl_4 solution at 0.01 M, whereas the monomer of 1-PhEtOH coexists with dimers and multimers in the CS_2 solution at 0.1 M.

VCD Spectra in Solutions and the Liquid State. The VCD spectrum of (–)-1-PhEtOH was measured in a CS_2 solution at 0.1 M, because the VCD measurements are generally difficult in a very dilute solution. Figure 8 shows the experimental VCD spectrum of (–)-1-PhEtOH, together with the calculated VCD spectra for the three conformers of (S)-1-PhEtOH. The spectrum calculated for conformer I reproduces fairly well the observed spectrum. The VCD bands observed at 1350, 1252, 1097, 1076, 1047, 994, and 899 cm^{-1} in the CS_2 solution are due to conformer I of (S)-1-PhEtOH. Thus, we identified that (–)-1-

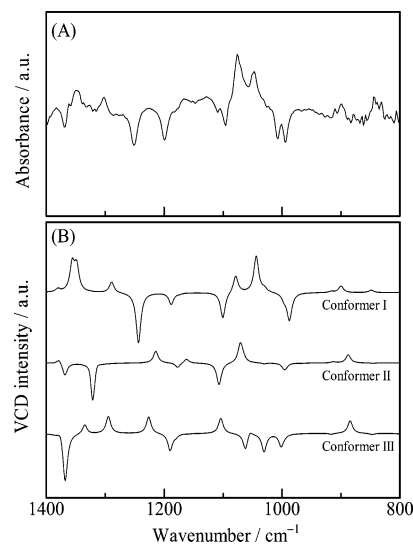


Figure 8. (A) VCD spectrum of (S)-(-)-1-PhEtOH observed in a CS_2 solution at 0.1 M. (B) Calculated VCD spectra for conformers I, II, and III.

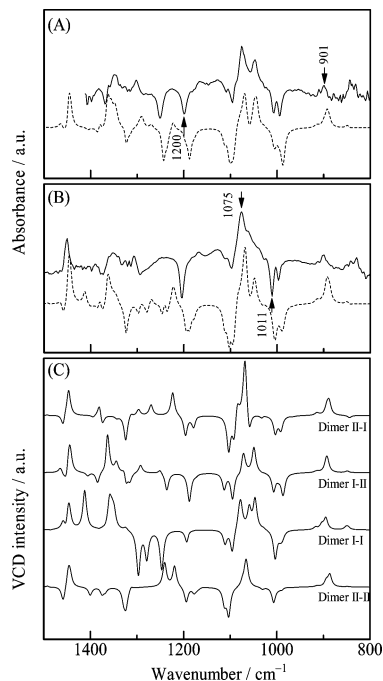


Figure 9. (A) Observed VCD spectrum of (S)-(-)-1-PhEtOH in a CS_2 solution at 0.1 M. The dotted line represents the population-weighted linear combination of the VCD spectra for the monomer and dimers, conformer I + dimer II–I + 0.5(dimer I–II). (B) Observed VCD spectrum of (S)-(-)-1-PhEtOH in the liquid state. The dotted line represents the population-weighted linear combination of the VCD spectra for the dimers, dimer II–I + dimer I–II + 0.5(dimer II–II + dimer I–I). (C) Calculated VCD spectra of the dimers I–II, II–I, I–I, and II–II.

PhEtOH is of S-configuration and exists predominantly as conformer I in a dilute CS_2 solution.

Figure 9, parts A and B, shows the comparison between the VCD spectrum of (–)-1-PhEtOH in the CS_2 solution at 0.1 M and that in the liquid state. The VCD spectrum in the solution is considerably different from that in the liquid state, especially in the 1120–1400 cm^{-1} region. The intermolecular H-bonding should cause this discrepancy. The COH bending mode, the CH deformation, and the C–C and CO stretching modes may

be largely perturbed by the formation of hydrogen bonds as anticipated from the ROA measurement; the calculated ROA spectrum is in excellent agreement with that observed in the liquid state in the region below 1120 cm^{-1} but is not matched in the $1120\text{--}1400\text{ cm}^{-1}$ region in which the bands are involved in OH bending modes.¹⁷ Then, VCD spectra of the (*S*)-1-PhEtOH dimers were calculated at the B3LYP/6-31G+(d,p) level in order to estimate the influence of intermolecular H-bonding on the VCD bands. By comparing the calculated VCD spectra in Figure 9C with those in Figure 8B, we found that the calculated spectra of the monomers and the dimers in the $1120\text{--}1400\text{ cm}^{-1}$ region are different from each other. These results indicate that the VCD spectra are largely influenced by both conformational changes and intermolecular H-bonding.

The population-weighted linear combination of the VCD spectra for the monomer and the dimers (conformer I + dimer II-I + 0.5(dimer I-II)) is in excellent agreement with that observed in a CS₂ solution at 0.1 M as shown in Figure 9A. The bands at 1200 and 1075 cm^{-1} , whose intensities increase in the liquid state, are associated with conformer II with the intermolecular OH...O H-bonding. On the other hand, the composite spectrum by dimer II-I + dimer I-II + 0.5(dimer II-II + dimer I-I) reproduces fairly well the VCD spectrum in the liquid state as shown in Figure 9B.

The result obtained here gives an insight into the method for analyzing a VCD spectrum observed for a concentrated solution or condensed phase. In general, VCD measurements for a very dilute solution, where no intermolecular H-bonding occurs, can clearly determine the absolute configuration of chiral molecules by comparing with the theoretical calculation for an isolated molecule. However, it is difficult in many cases to detect clear VCD signals for a very dilute solution. As demonstrated in the present work, it is very practical to find a key VCD band that is insensitive to both the conformational changes and the intermolecular H-bonding for determining the absolute configuration of chiral molecules in a concentrated solution. In the case of (-)-1-PhEtOH, the VCD bands at 1011 and 901 cm^{-1} , which are due to the C=C stretching and CH bending (*ip*) of the phenyl ring, respectively, are the key bands. To identify the key VCD bands enables us to determine the absolute configuration of chiral molecules even in the condensed phases such as the liquid state.

This methodology may be applicable to the investigation of large molecules in biological system. For finding key bands that are insensitive to both the conformational changes and the intermolecular H-bonding, the computational analysis is a powerful tool. In order to estimate the influence of intermolecular H-bonding on a VCD band, a direct interaction such as O-H...O or N-H...N interactions should be considered in simulations. As demonstrated in this work, a complicated experimental VCD spectrum may be understandable by a linear combination of calculated spectra obtained for several possible conformers or compounds. This pattern-matching scenario enables us to analyze a VCD spectrum of much larger molecules by means of a linear combination of VCD spectra simulated for certain fragments.

Conclusions

The absolute configuration and conformation of 1-phenylethanol (1-PhEtOH) have been investigated by matrix-isolation IR and VCD spectroscopy combined with quantum chemical calculations. Local minima of (*S*)-1-PhEtOH were found by calculating 2-D potential-energy surface map at the HF/6-31G-(d,p) level. Three conformers at the local minima were optimized

at the B3LYP/6-311++G(d,p) level. The calculated IR spectrum of conformer I reproduces very well the Ar matrix-isolation IR spectrum. The quantum chemical calculation revealed that conformer I is stabilized by both intramolecular CH...O and O-H... π H-bonding. In dilute CCl₄ and CS₂ solutions, 1-PhEtOH exists predominantly as conformer I with a trace amount of conformer II. In the liquid state of 1-PhEtOH, conformer II is stabilized by intermolecular OH...O H-bonding and coexists with conformer I.

By considering conformations and intermolecular H-bonding, we successfully reproduced the observed VCD spectra. The absolute configuration of (-)-1-PhEtOH in a dilute CS₂ solution is determined to be *S*-configuration. The population-weighted linear combination of the VCD spectra for the monomer and the dimers is in excellent agreement with that observed in a CS₂ solution at 0.1 M, while the composite spectrum for the dimers reproduces fairly well the VCD spectrum in the liquid state. The result indicated that the difference of the VCD spectra between the dilute solution and the liquid state arises not only from conformational changes but also from the intermolecular H-bonding. Thus, we concluded that the determination of the absolute configuration of 1-PhEtOH in condensed phases is enabled by identifying VCD bands that are insensitive to conformational changes and intermolecular interactions. In the present work, we have also demonstrated that a complicated experimental VCD spectrum is understandable by a linear combination of calculated spectra obtained for several possible conformers or compounds. This pattern-matching scenario may enable us to analyze a VCD spectrum of much larger molecules by means of a linear combination of VCD spectra simulated for certain fragments.

Acknowledgment. This work was partially supported by a Grant-in-Aid for Scientific Research (No. 16205003) from the Ministry of Education, Culture, Sports, Science, and Technology (MEXT) of the Japanese Government.

Supporting Information Available: Coordinates and harmonic vibrational wavenumbers of the dimers for 1-phenylethanol, comparison between the optimized structures for conformers obtained at the B3LYP/6-31+G(d,p) level and those at the MP2/6-31+G(d,p) level, comparison among the optimized structures of conformers obtained by the IEF-PCM method at the B3LYP/6-31+G(d,p) level of calculations in vacuo, in CCl₄, and in methanol. This material is available free of charge via the Internet at <http://pubs.acs.org>.

References and Notes

- (1) Freedman, T. B.; Cao, X.; Dukor, R. K.; Nafie, L. A. *Chirality* **2003**, *15*, 743.
- (2) Jeffrey, G. A.; Saenger, W. *H-Bonding in Biological Structures*; Springer: Berlin, 1994.
- (3) Yoshida, H.; Kaneko, I.; Matsuura, H.; Ogawa, Y.; Tasumi, M. *Chem. Phys. Lett.* **1992**, *196*, 601.
- (4) Jaffe, R. L.; Smith, G. D.; Yoon, D. Y. *J. Phys. Chem.* **1993**, *97*, 12745.
- (5) Yoshida, H.; Harada, T.; Ohno, K.; Matsuura, H. *Chem. Commun.* **1997**, 2213.
- (6) Ohno, K.; Tonegawa, A.; Yoshida, H.; Matsuura, H. *J. Mol. Struct.* **1993**, *299*, 141.
- (7) Ohno, K.; Matsumoto, H.; Yoshida, H.; Matsuura, H.; Iwaki, T.; Suda, T. *J. Phys. Chem. A* **1998**, *41*, 8056.
- (8) Voet, D.; Voet, J. G. *Biochemistry*, 2nd ed.; Wiley: New York, 1995.
- (9) (a) Nafie, L. A.; Peticolas, W. L. *J. Chem. Phys.* **1972**, *57*, 3145-3155. (b) Nafie, L. A.; Diem, M.; Vidrine, D. W. *J. Am. Chem. Soc.* **1979**, *101*, 496-498. (c) Polavarapu, P. L.; Nafie, L. A. *J. Chem. Phys.* **1980**, *73*, 1567.

- (10) (a) Sen, A. C.; Keiderling, T. A. *Biopolymers* **1984**, 23, 1533. (b) Pancoska, P.; Keiderling, T. A. *Biochemistry* **1991**, 30, 6885. (c) Baumruk, V.; Keiderling, T. A. *J. Am. Chem. Soc.* **1993**, 115, 6939.
- (11) (a) Nakao, Y.; Sugeta, H.; Kyogoku, Y. *Chem. Lett.* **1984**, 4, 623. (b) Miyazawa, M.; Kyogoku, Y.; Sugeta, H. *Spectrochim. Acta, Part A* **1994**, 50A, 1505. (c) Nakao, K.; Kyogoku, Y.; Sugeta, H. *Faraday Discuss.* **1995**, 99, 77.
- (12) Harada, T.; Yoshida, H.; Ohno, K.; Matsuura, H. *J. Phys. Chem. A* **2001**, 105, 4517.
- (13) Yoshida, H.; Harada, T.; Murase, T.; Ohno, K.; Matsuura, H. *J. Phys. Chem. A* **1997**, 101, 1731.
- (14) Matsuura, H.; Yoshida, H.; Hieda, M.; Yamanaka, S.; Harada, T.; Shin-ya, K.; Ohno, K. *J. Am. Chem. Soc.* **2003**, 125, 13910.
- (15) Giardini Guidoni, A.; Piccirillo, S.; Scuderi, D.; Satta, M.; Di Palma, T. M.; Speranza, M. *Phys. Chem. Chem. Phys.* **2000**, 2, 4139.
- (16) Barbu, K. L.; Lahmani, F.; Mons, M.; Broquier, M.; Zehnacker, A. *Phys. Chem. Chem. Phys.* **2001**, 3, 4684.
- (17) Macleod, N. A.; Butz, P.; Simons, J. P.; Grant, G. H.; Baker, C. M.; Tranter, G. E. *Phys. Chem. Chem. Phys.* **2005**, 7, 1432.
- (18) Macleod, N. A.; Butz, P.; Simons, J. P.; Grant, G. H.; Baker, C. M.; Tranter, G. E. *Isr. J. Chem.* **2004**, 44, 27.
- (19) Frisch, M. J.; Trucks, G. W.; Schlegel, H. B.; Scuseria, G. E.; Robb, M. A.; Cheeseman, J. R.; Zakrzewski, V. G.; Montgomery, J. A., Jr.; Stratmann, R. E.; Burant, J. C.; Dapprich, S.; Millam, J. M.; Daniels, A. D.; Kudin, K. N.; Strain, M. C.; Farkas, O.; Tomasi, J.; Barone, V.; Cossi, M.; Cammi, R.; Mennucci, B.; Pomelli, C.; Adamo, C.; Clifford, S.; Ochterski, J.; Petersson, G. A.; Ayala, P. Y.; Cui, Q.; Morokuma, K.; Malick, D. K.; Rabuck, A. D.; Raghavachari, K.; Foresman, J. B.; Cioslowski, J.; Ortiz, J. V.; Stefanov, B. B.; Liu, G.; Liashenko, A.; Piskorz, P.; Komaromi, I.; Gomperts, R.; Martin, R. L.; Fox, D. J.; Keith, T.; Al-Laham, M. A.; Peng, C. Y.; Nanayakkara, A.; Gonzalez, C.; Challacombe, M.; Gill, P. M. W.; Johnson, B.; Chen, W.; Wong, M. W.; Andres, J. L.; Gonzalez, C.; Head-Gordon, M.; Replogle, E. S.; Pople, J. A. *Gaussian 98*, revision A.5; Gaussian, Inc.: Pittsburgh, PA, 1998.
- (20) (a) Becke, A. D. *J. Chem. Phys.* **1993**, 98, 5648–5652. (b) Lee, C.; Yang, W.; Parr, R. G. *Phys. Rev. B* **1988**, 37, 785.
- (21) (a) Head-Gordon, M.; Pople, J. A.; Frisch, M. J. *Chem. Phys. Lett.* **1988**, 153, 503. (b) Frisch, M. J.; Head-Gordon, M.; Pople, J. A. *Chem. Phys. Lett.* **1990**, 166, 275. (c) Frisch, M. J.; Head-Gordon, M.; Pople, J. A. *Chem. Phys. Lett.* **1990**, 166, 281. (d) Head-Gordon, M.; Head-Gordon, T. *Chem. Phys. Lett.* **1994**, 220, 122. (e) Saebo, S.; Almlöf, J. *Chem. Phys. Lett.* **1989**, 154, 8.
- (22) (a) Cancès, M. T.; Mennucci, B.; Tomasi, J. *J. Chem. Phys.* **1997**, 107, 3032. (b) Cossi, M.; Barone, V.; Mennucci, B.; Tomasi, J. *Chem. Phys. Lett.* **1998**, 286, 253. (c) Mennucci, B.; Tomasi, J. *J. Chem. Phys.* **1997**, 106, 5151.
- (23) Curtiss, L. A.; Raghavachari, K.; Pople, J. A. *J. Chem. Phys.* **1993**, 98, 1293.
- (24) Yoshida, H.; Ehara, A.; Matsuura, H. *Chem. Phys. Lett.* **2000**, 325, 477.
- (25) Caminati, W.; Daminani, D. *Mol. Phys.* **1991**, 74, 885.
- (26) Mons, M.; Robertson, E. G.; Simons, J. P. *J. Phys. Chem. A* **2000**, 104, 1430.
- (27) See Figure S1 in the Supporting Information.
- (28) Optimized structures are found in Figure S2 in the Supporting Information.
- (29) Hobza, P.; Havlas, Z. *Chem. Phys. Lett.* **1999**, 303, 447.
- (30) Maté, B.; Suenram, R. D.; Lugez, C. *J. Chem. Phys.* **2000**, 113, 192.
- (31) Felder, P.; Günthard, H. H. *Spectrochim. Acta, Part A* **1980**, 36, 223.
- (32) Kudoh, S.; Takayanagi, M.; Nakata, M. *Chem. Phys. Lett.* **1998**, 296, 329.
- (33) Barnes, A. J. *J. Mol. Struct.* **1984**, 113, 161.
- (34) Oki, M.; Iwamura, H. *Bull. Chem. Soc. Jpn.* **1959**, 32, 950.
- (35) Davies, M. *Infrared Spectroscopy and Molecular Structures*; Elsevier: Amsterdam, 1963.
- (36) Kurita, E.; Matsuura, H.; Ohno, K. *Spectrochim. Acta, Part A* **2004**, 60, 3005.
- (37) (a) Ohno, K.; Okimura, M.; Akai, N.; Katsumoto, Y. *Phys. Chem. Chem. Phys.* **2005**, 7, 3005. (b) Ohno, K.; Takao, H.; Masuda, T.; Katsumoto, Y. *Chem. Lett.* **2005**, 34, 250.
- (38) Levering, L. M.; Hayes, C. J.; Callahan, K. M.; Hadad, C. M.; Allen, H. C. *J. Phys. Chem.* **2006**, 110, 6325.
- (39) SDBSWeb. <http://www.aist.go.jp/RIODB/SDBS/> (National Institute of Advanced Industrial Science and Technology, accessed May, 2006).